JACS
JOURNAL OF THE AMERICAN CHEMICAL SOCIETY

Article

Chiral Phosphoric Acid-Catalyzed Enantioselective Ring Expansion Reaction of 1,3-Dithiane Derivatives: Case Study of the Nature of Ion-Pairing Interaction

Feng Li, Toshinobu Korenaga, Taishi Nakanishi, Jun Kikuchi, and Masahiro Terada

J. Am. Chem. Soc., **Just Accepted Manuscript** • DOI: 10.1021/jacs.7b13274 • Publication Date (Web): 29 Jan 2018

Just Accepted

ACS Publications

Journal of the American Chemical Society is published by the American Chemical Society. 1155 Sixteenth Street N.W., Washington, DC 20036

Chiral Phosphoric Acid-Catalyzed Enantioselective Ring Expansion Reaction of 1,3-Dithiane Derivatives: Case Study of the Nature of Ion-Pairing Interaction

Feng Li,[†] Toshinobu Korenaga,[§] Taishi Nakanishi,[†] Jun Kikuchi,[†] Masahiro Terada*[,†]

† Department of Chemistry, Graduate School of Science, Tohoku University, Aoba-ku, Sendai 980-8578, Japan

§ Department of Chemistry and Biological Sciences, Faculty of Science and Engineering, Iwate University, 4-3-5 Ueda, Morioka 020-8551, Japan

ABSTRACT: Chiral counter ion controlled asymmetric catalysis via an ion-pairing interaction has attracted immense attention in recent years. Despite a number of successful studies, the mechanistic elucidation of the stereocontrolling element in the ion-pairing interaction is rarely conducted and hence its nature is still far from being well understood. Herein we report an in-depth mechanistic case study of a newly developed enantioselective ring expansion reaction of 1,3-dithiane derivatives catalyzed by chiral phosphoric acid (CPA). An unprecedented enantioselective 1,2-sulfur rearrangement/stereospecific nucleophilic addition sequence was proven to be the stereoselective pathway. More importantly, by thorough investigation of the intrinsic nature of the stereospecific nucleophilic addition to the cationic thionium intermediate, we discovered that the key interaction in this process is the non-classical C-H···O hydrogen bonds formed between the conjugate base of the CPA catalyst and the cationic intermediate. These C-H···O hydrogen bonds not only bind the catalyst to the substrates to form energetically favored states throughout the overall processes, but also firmly maintain the relative positions of these fragments as the "fixed" contact ion pair to sustain the chiral information generated at the initial sulfur rearrangement step. This mechanistic case study provides a very clear understanding of the nature of the ion-pairing interaction in organocatalysis. The conclusion encourages the further development of the research field with an eye to designing new organocatalysts and cultivating novel organocatalytic transformations.

INTRODUCTION

The chiral anion controlled asymmetric catalysis *via* an ion-pairing interaction in organic synthesis has drawn much attention in recent years.[1] Chiral phosphate anion, particularly the one derived from the BINOL backbone (BINOL = 1,1'-bi-2-naphthol), is one of the most widely used chiral anions in enantioselective transformations. It is the conjugate base of chiral phosphoric acid (CPA), a powerful and versatile chiral Brønsted acid catalyst used in numerous enantioselective reactions (Figure 1).[2] The activation mode in the CPA-catalyzed reactions of electronically neutral substrates is well recognized through the double hydrogen-bonding interaction: the Brønsted acidic site (P-O<u>H</u>) interacts with an electrophile (e.g., imine, aldehyde, etc.) to form a hydrogen bond of O···H···X (X = NR, O, etc.) and the Brønsted basic site of phosphoryl oxygen (P=<u>O</u>) simultaneously forms a hydrogen bond with a nucleophile (Figure 1a).[2] In sharp contrast, a similar hydrogen bond cannot be clearly identified in the ion-pairing interaction due to the lack of an H-X moiety, an active proton attached to a heteroatom, in cationic species (Figure 1b). In spite of the large number of successful examples, mechanistic studies of this type of reaction are rare. Our research group has disclosed that the non-classical C-H···O hydrogen bonds between an oxocarbenium ion and a chiral phosphate anion are crucial to achieving a high level of stereocontrol in a CPA-catalyzed Petasis-Ferrier-type rearrangement.[3] To better understand the nature of the ion-pairing interaction in asymmetric catalysis, further studies of different types of stereoselective transformations involving the cationic species as a reactive intermediate are keenly required.

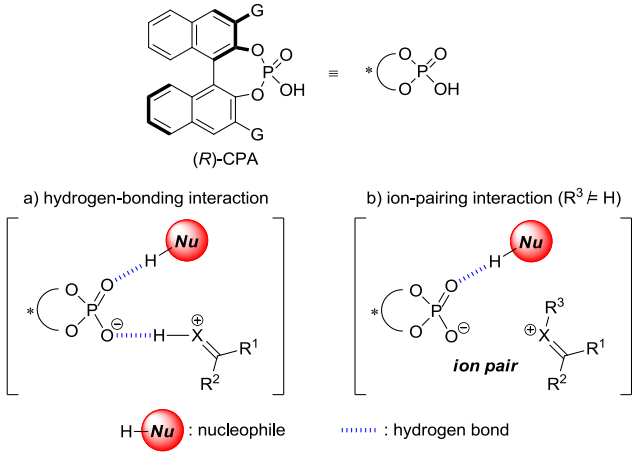

Figure 1. Activation mode of CPA-catalyzed reaction.

The thionium ion is a representative sulfur-stabilized carbocation and the sulfur analog of oxocarbenium ion. It is widely found as a reactive intermediate in a variety of reactions, such as the Pummerer rearrangement and related reactions.[4] However, the catalytic enantioselective reactions of thionium to furnish enantio-enriched sulfur-containing compounds remain largely unexplored.[5] In this context, we envisioned that chiral phosphate would be applicable as a counter anion of the thionium intermediate to control the stereochemical outcome in an enantioselective fashion. The method provides a new entry into the catalytic asymmetric synthesis of enantio-enriched sulfur-containing compounds.[6] More importantly, the thionium

functionality possesses no H-X (X = sulfur) moiety to form hydrogen bonds and hence, a thorough mechanistic study would offer some insights into stereocontrolling elements in the ion-pairing interaction.

To accomplish the proposed enantioselective transformation involving the thionium intermediate, we focused our attention on the 1,2-sulfur rearrangement of dithio-acetal or -ketal derivatives with a leaving group at the α-position (Scheme 1a).[7] The conventionally assumed mechanism is as follows. At first, a nucleophilic attack by sulfur atom initiates a substitution reaction at the α-carbon with the elimination of the leaving group, affording a meta-stable episulfonium ion. The episulfonium ion undergoes ring opening immediately to generate a thionium ion *via* the 1,2-sulfur rearrangement. Finally, the thionium ion is trapped by a nucleophile to afford an addition product or undergoes deprotonation to yield an alkene (elimination) product.

Scheme 1. Reaction of thionium ion generated by 1,2-sulfur rearrangement.

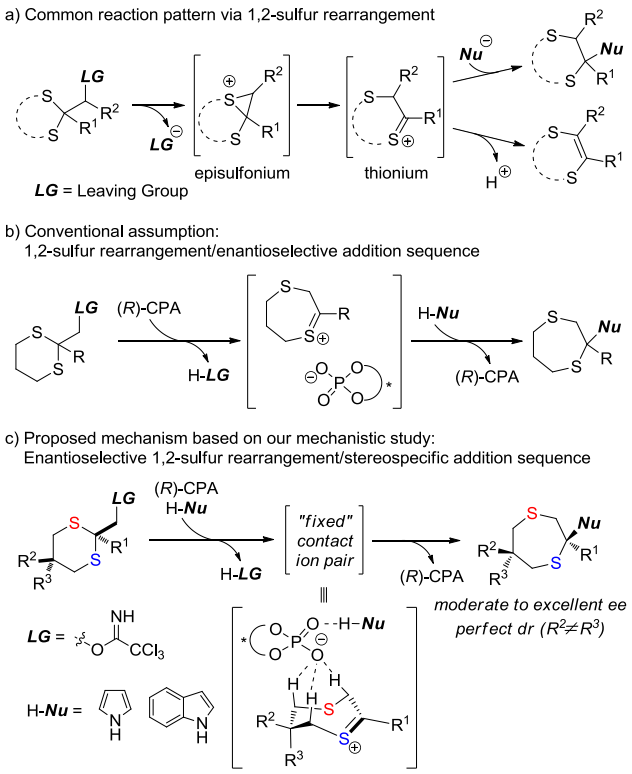

On the basis of conventional assumption,[7] 1,3-dithiane derivative undergoes the 1,2-sulfur rearrangement *via* the activation of the leaving group by CPA catalyst to generate an ion pair intermediate consisting of chiral phosphate and achiral thionium ion (Scheme 1b). It is assumed that under the influence of chiral phosphate, the following nucleophilic addition would take place in an enantioselective manner to afford an enantio-enriched 1,4-dithiepane product. However, our mechanistic case study revealed that the reaction proceeds through an unprecedented enantioselective 1,2-sulfur rearrangement/stereospecific nucleophilic addition sequence (Scheme 1c). Notably, the present stereospecific addition is enabled by the non-classical C-H···O hydrogen bonding interaction between the catalyst and the substrate. The C-H···O hydrogen bonds not only allow the formation of energetically favored states between the substrate and the catalyst throughout the overall processes, but also firmly maintain their relative positions to form a "fixed" contact ion pair. Hence, the chiral information generated at the initial sulfur rearrangement step remains unchanged during the course of the addition step. Herein we report our journey toward the discovery of this novel enantioselective transformation and the results of our comprehensive mechanistic case study.

RESULTS AND DISCUSSION

Substituent effect of 1,3-dithiane derivative

After an extensive screening process, the reaction conditions were optimized as follows:[8] 1,3-dithiane derivative **2** with a trichloroacetimidate group at the α-position was used as the substrate.[9] The reaction was performed with 1.5 equivalents of pyrrole (**3a**) and 10 mol % of (*R*)-**1a**[10] as CPA in dichloromethane at -40 ºC for 12 h.

With the optimized reaction conditions in hand, the substituent effect of the substrate was tested (Table 1). As expected, the yield of product **4** was dependent on the electronic property of substituent R^1 at the 2-position of 1,3-dithiane **2**: the substitution by an electron-donating group (EDG) resulted in a higher yield than that by an electron-withdrawing group (EWG) because of the stabilization of the cationic thionium intermediate by EDG (Table 1, **4a-g**).[11] In contrast, it is noteworthy that the enantioselectivities were comparable even when the electronic property of aromatic substituent R^1 was changed, affording **4** with around 80% ee in all cases (**4a-g**). The absolute configuration of the product was determined to be (*R*) by the single-crystal X-ray diffraction analysis of **4f**.[12] Switching substituent R^1 to an aliphatic *n*-propyl group gave product **4h** in moderate yield with a slight reduction of enantioselectivity (74% ee). The introduction of geminal substituents at the 5-position of 1,3-dithiane led to a significant increase in enantioselectivity (**4i** and **4j**). It should be underscored that the substituents ($R^2 = R^3 \neq H$) at the 5-position markedly influence enantioselectivity compared to substituent R^1 at the 2-position, despite the fact that substituents R^2 and R^3 at the 5-position are located far from the reaction site.

Table 1. Substituent effect of 1,3-dithiane derivatives 2.[a]

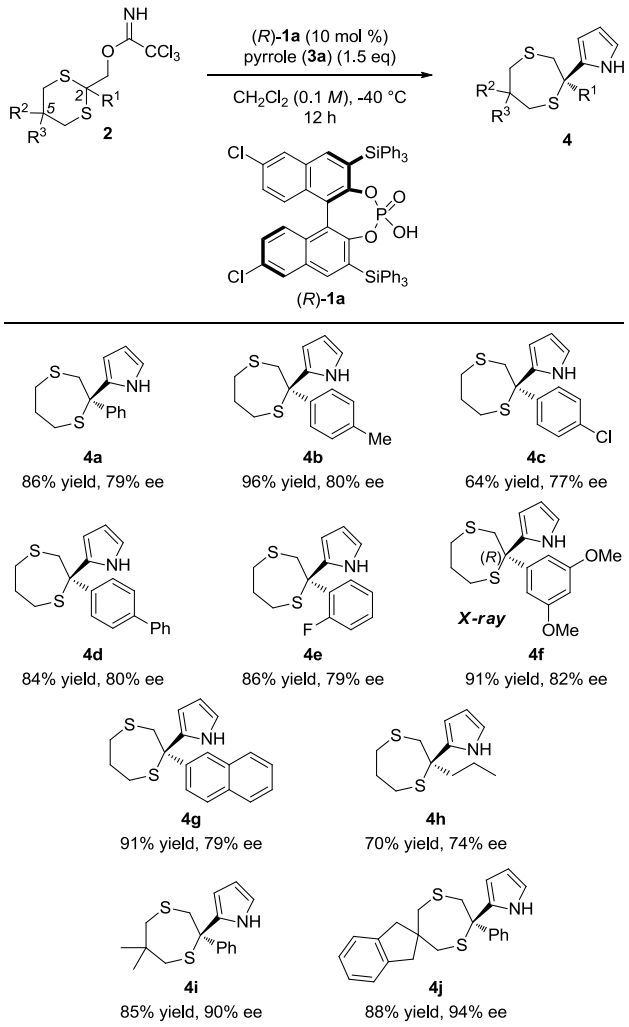

[a] All reactions were carried out using 0.01 mmol of (*R*)-**1a** (10 mol %), 0.1 mmol of 1,3-dithiane derivative **2**, and 0.15 mmol of pyrrole **3a** (1.5 equiv) in dichloromethane (1.0 mL, 0.1 *M*) at -40 °C for 12 h.

To further investigate the substituent effect at the 5-position of substrate **2**, *cis/trans* isomers **2k** and **2l** having a monobenzyl substituent were tested under the optimized reaction conditions (Scheme 2).[13] From geometrically single **2k**, product **4k** was obtained in good yield with perfect diastereoselectivity and excellent enantioselectivity (Scheme 2a, condition 1). The absolute configuration of **4k** was unambiguously determined to be (2*R*, 6*S*) by single-crystal X-ray diffraction analysis.[12] From geometrically single **2l**, diastereomer **4l** was obtained as the sole product.[14] However, the reactivity of **2l** was much lower than that of **2k**; the conversion of **2l** was only 56% after 12 h (Scheme 2b, condition 1). Moreover, the enantiomeric excess of **4l** (79% ee) was much lower than that of **4k** (97% ee) and was identical to that of **4a** (79% ee) obtained from **2a** that had no substituent at the 5-position of 1,3-dithiane (Table 1). These results clearly indicate that the substituent at the 5-position *cis* to the leaving group significantly enhances the enantioselectivity, whereas the substituent *trans* to the leaving group has nearly no effect on the enantioselectivity. Further optimization of the reaction conditions by using molecular sieve (MS) 4A resulted in nearly perfect yields and diastereoselectivities for both **4k** and **4l** without marked loss of enantioselectivity (Schemes 2a and 2b, condition 2).

Scheme 2. Reactions of 1,3-dithiane derivatives having mono-substituent at 5-position.

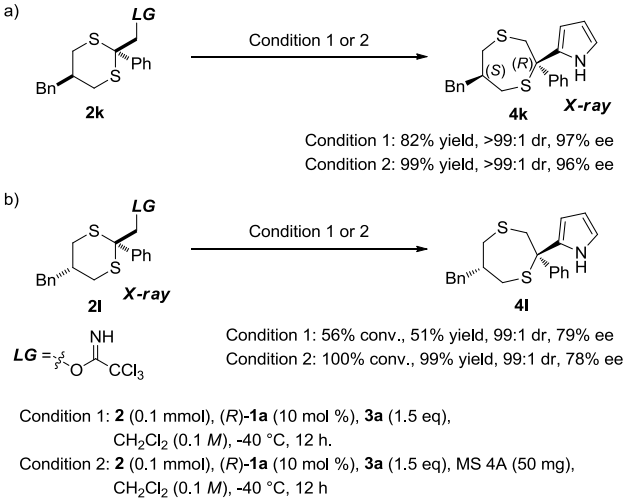

Condition 1: **2** (0.1 mmol), (*R*)-**1a** (10 mol %), **3a** (1.5 eq), CH_2Cl_2 (0.1 *M*), -40 °C, 12 h.
Condition 2: **2** (0.1 mmol), (*R*)-**1a** (10 mol %), **3a** (1.5 eq), MS 4A (50 mg), CH_2Cl_2 (0.1 *M*), -40 °C, 12 h

Mechanistic study-1: Is nucleophilic addition the enantio-determining step (EDS)?

In the course of our investigation of the substituent effect in this reaction, we uncovered two intriguing features: 1) enantioselectivity is markedly dependent on the substituent at the 5-position *cis*/*trans* to the leaving group; 2) the reactions of **2k** and **2l** yield different diastereomeric products with excellent dr values. In other words, the reaction is stereospecific. These results encouraged us to further investigate the reaction mechanism. The most important issue is whether an enantioselective addition to thionium takes place under the influence of a chiral phosphate counter ion, as shown in Scheme 1b. To verify this issue, we conducted two control experiments.

In the first control experiment, we used a substrate having a different leaving group. We hypothesized that if the addition to thionium ion paired with chiral phosphate were the enantiodetermining step (EDS), the enantioselectivity of the product would be the same irrespective of the leaving group. That is because the leaving group is not involved in the nucleophilic addition step. With this hypothesis in mind, *N*-phenyl trifluoroacetimidate [5b] was selected as the leaving group. The reaction of **5d**[12,15] having an *N*-phenyl trifluoroacetimidate moiety was conducted at room temperature for 4 h.[16] As a result, (*S*)-**4d** was obtained in 17% yield with 11% ee along with alkene byproduct **6d** (Scheme 3a). In contrast, substrate **2d** was completely consumed within 1 h under the same conditions and (*R*)-**4d** was obtained in 88% yield with 44% ee (Scheme 3b). **4d** enantiomers with different enantioselectivities were the major products obtained from **2d** and **5d**. These results strongly suggest that nucleophilic addition to thionium is not the EDS of this reaction.

Scheme 3. Reactions of 1,3-dithiane derivatives having different leaving groups.

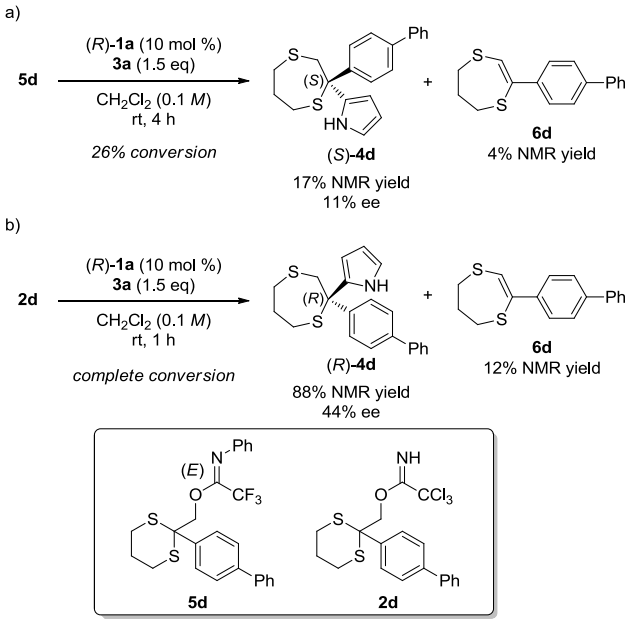

In the second control experiment, we performed the reactions using **2k** and **2l** in the presence of achiral acid catalyst **1b** without a substituent at the *ortho*-position of the phenol group. We hypothesized that if the ion pair depicted in Scheme 1b were the plausible intermediate, an identical ion pair would be generated from **2k** and **2l** using **1b** and this would result in the formation of products with the same dr value (Scheme 4, Path I). Otherwise, as observed in the reaction using **1a**, **4k** and **4l** would be formed from **2k** and **2l**, respectively, in a stereospecific manner, regardless of the steric congestion around the phosphoric acid functionality (Scheme 4, Path II).

Scheme 4. Plausible mechanisms with achiral catalyst.

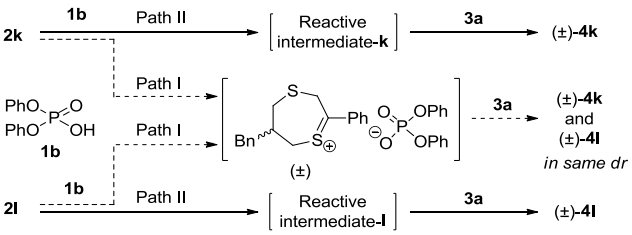

The reactions of **2k** and **2l** were carried out with 10 mol % of achiral phosphoric acid **1b** and 1.5 equivalents of pyrrole **3a** in dichloromethane at 0 ºC for 2 h. As shown in Scheme 5, racemic **4k** and **4l** were formed from **2k** and **2l**, respectively, in high yields with excellent dr values. These results clearly indicate that the substituents at the 3,3'-positions of BINOL-derived CPA are not essential for the specific formation of **4k** and **4l** in excellent diastereoselectivity. More importantly, the ion pair depicted in Scheme 1b (see also Scheme 4, Path I), which was assumed from a number of previous reports,[7] is not suited as the plausible intermediate in this reaction. The reactions of **2k** and **2l** should proceed *via* "well-ordered" intermediates because of the stereospecific process (Scheme 4, Path II).

Scheme 5. Reactions using achiral catalyst.

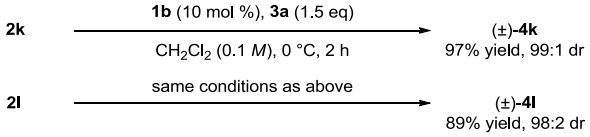

Considering the stereochemical relationship between **2k** and **4k** as well as **2l** and **4l**, it is clear that the nucleophilic addition of pyrrole **3a** to thionium proceeds exclusively on the same side of the cyclic framework with the leaving group in a stereospecific manner. Consequently, the direction of the addition reaction is unambiguously determined by the location of the leaving group. The above consideration coupled with the results obtained by changing the leaving group (Scheme 3) leads to a solid outline of the overall process: the addition step is not EDS and hence the initial step, 1,2-sulfur rearrangement, should be EDS (Scheme 6). Indeed, the estimated outline is consistent with the experimental evidence that enantioselectivity changes dramatically when the substrate leaving group is switched, because the leaving group is involved in the initial step. 1,3-Dithiane substrates **2** are achiral molecules; however, the two sulfur atoms are enantiotopic (shown in red and blue). Therefore, it can be proposed that CPA differentiates these two enantiotopic sulfur atoms and the rearrangement of one sulfur atom (shown in red) is more favorable than that of the other (shown in blue). After the selective sulfur rearrangement, two reactive and "well-ordered" intermediates are generated with one being the major intermediate. Subsequent addition to these intermediates proceeds in a stereospecific manner, and both major and minor intermediates are transformed into the corresponding major and minor products. The ratio of the two intermediates should be equal to the enantiomeric ratio of final product **4**.

Scheme 6. Proposed revised mechanism with CPA.

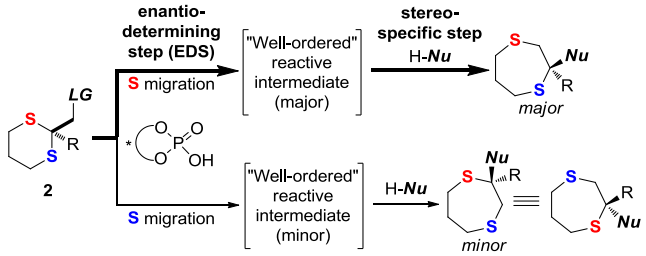

Mechanistic study-2: Reaction with different nucleophiles.

In the previous section, it was proposed that the 1,2-sulfur rearrangement step should be EDS. It can be considered that in principle, enantioselectivity should be determined irrespective of the nucleophile employed, because only the substrate and CPA are involved in this step (Scheme 6). On the basis of this working hypothesis of EDS, coupled with the subsequent stereospecific addition, products with the same ee value should be obtained even when different nucleophiles are used (Scheme 7).

Scheme 7. Hypothesis: different nucleophiles give products with the same ee.

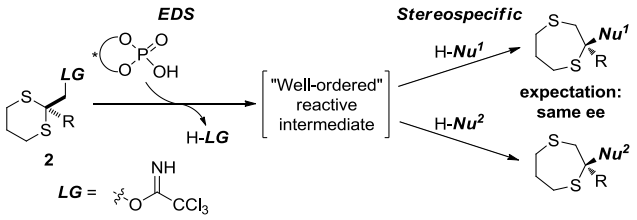

To validate our hypothesis, indole (**3b**) was employed as the nucleophile because of the similarity in reactivity of indole (**3b**) and pyrrole (**3a**). As shown in Table 2, the reaction of indole (**3b**) (1.5 equiv.) was performed with five 1,3-dithiane derivatives **2** using 5 mol % of optimized CPA catalyst (*R*)-**1a** at -40 ºC for 6 h. Analogous products **7** were obtained in excellent yields. However, it is noteworthy that the enantiomeric excess of all the five products **7** was obviously lower than that of the corresponding products **4** derived from pyrrole (**3a**) (Table 2 vs. Table 1). This result is not consistent with our hypothesis that products with the same enantioselectivity would be formed even if the nucleophile was changed, as shown in Scheme 7.

Table 2. Reactions of 1,3-dithiane derivatives with indole.[a]

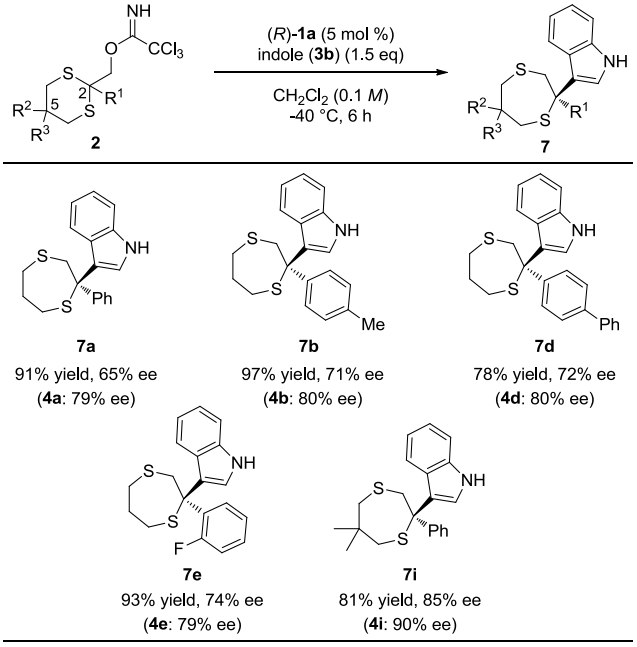

[a] All reactions were carried out using 0.005 mmol of (*R*)-**1a** (5 mol %), 0.1 mmol of 1,3-dithiane derivative **2**, and 0.15 mmol of indole (**3b**) (1.5 equiv) in dichloromethane (1.0 mL, 0.1 *M*) at -40 °C for 6 h. Ee values of corresponding **4** are shown in parentheses.

Before discussing this contradiction, to ascertain that the nucleophilic attack by indole (**3b**) is stereospecific, we conducted the reactions using substrates **2k** and **2l** under the optimized reaction conditions. As shown in Scheme 8, products **7k** and **7l** were formed from **2k** and **2l**, respectively, in excellent yields with perfect diastereoselectivity and hence the reaction of indole (**3b**) is also stereospecific.[14] In addition, the ee value of **7k** was much higher than that of **7l**, similar to that observed in the reaction of pyrrole (**3a**) (Scheme 2). Further analysis of these diastereomeric products showed that the ee value of **7k** (Scheme 8a: 95% ee) was slightly lower than that of **4k** (Scheme 2a: 96% ee), whereas **7l** (Scheme 8b: 73% ee) had an obviously lower ee than **4l** (Scheme 2b: 78% ee).

Scheme 8. Reactions of 2k and 2l with indole.

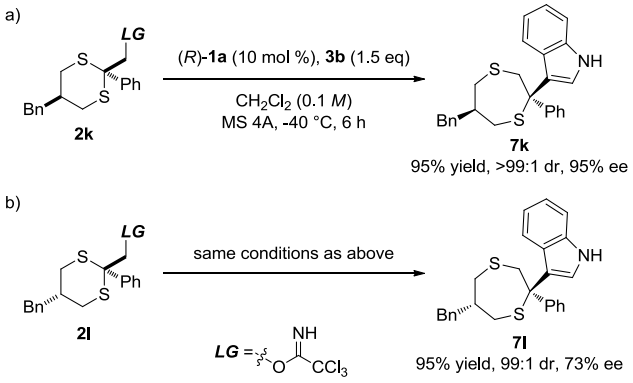

From the results of these diastereomeric products as well as those shown in Table 1 [pyrrole (**3a**)] and Table 2 [indole (**3b**)], it can be concluded that enantioselectivity is dependent on the nucleophile employed even though the reaction proceeds in a stereospecific manner. It implies that further amendment of the mechanism proposed in Scheme 6 is necessary to rationalize the stereochemical outcome governed by nucleophiles. A plausible mechanism is that the nucleophile is involved in EDS, because the nucleophile is the only differing factor in these reactions (Scheme 9). Based on the dual activation mode of CPA (Figure 1a), it is considered that the Brønsted acidic site of CPA activates the leaving group, trichloroacetimidate, in the initial step of this reaction. Meanwhile, a hydrogen bond is formed between the Brønsted basic site of CPA, the phosphoryl oxygen, and N-H moiety of pyrrole or indole nucleophile (Scheme 9), which would stabilize the phosphate anion generated by the protonation of the leaving group. Subsequently, the 1,2-sulfur rearrangement occurs under the chiral environment created by CPA that bears the nucleophile through the hydrogen bond.[17] This would rationalize why pyrrole and indole gave products with different enantioselectivities.

Scheme 9. Further amended mechanism and proposed EDS.

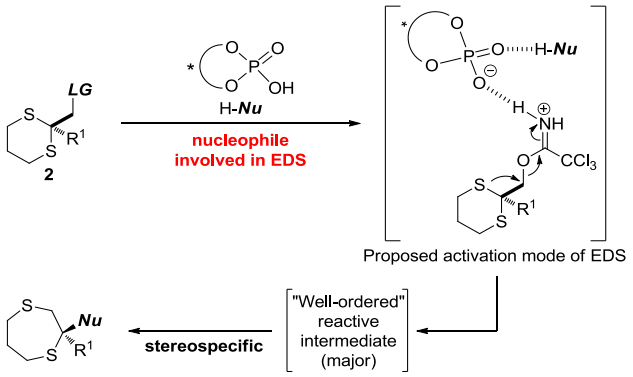

Mechanistic study-3: reaction without nucleophile or with *N*-Me-pyrrole and *N*-Me-indole as nucleophile

As proposed in the previous section, pyrrole and indole are involved in EDS by forming a hydrogen bond with phosphoryl oxygen. In order to verify this interaction,[17] we excluded the hydrogen bond from the reaction system in which reactions

were performed without a nucleophile or by using an *N*-methyl substituted pyrrole and indole as the nucleophile.

Based on our examination of previous reports,[7] we expect that a ring expansion/deprotonation product would be formed in the absence of a nucleophile (Scheme 1a). The reaction of **2k** or **2l** in the absence of nucleophile affords the corresponding elimination product in an enantioselective manner because of the generation of the stereogenic center at the 6-position, which reflects the chiral information of EDS. The enantioselectivity of these products may offer some clues to help us determine to what extent pyrrole and indole affect the enantioselectivity of EDS.

The reaction of **2k** and **2l** in the absence of nucleophile was carried out using 10 mol % of optimized catalyst (*R*)-**1a** and MS 4A at -40 ºC for 12 h. As shown in Scheme 10, ring expansion/deprotonation product **6k** was obtained from **2k** and **2l** with 96% ee (*S*) and 79% ee (*R*), respectively.[14] In the reaction of **2k**, the ee value of (*S*)-**6k** (96% ee) is the same as that of **4k** (96% ee) and slightly higher than that of **7k** (95% ee) (Schemes 10a, 2a, and 8a). Likewise in the reaction of **2l**, upon comparing the enantioselectivities of (*R*)-**6k** (79% ee), **4l** (78% ee), and **7l** (73% ee) (Schemes 10b, 2b, and 8b), it became clear that the addition of indole (**3b**) resulted in an obvious decrease in enantioselectivity. It can be concluded that indole (**3b**) influences the ee values, whereas pyrrole (**3a**) has little effect.

Scheme 10. Reactions of 2k and 2l without nucleophile (H-*Nu*).

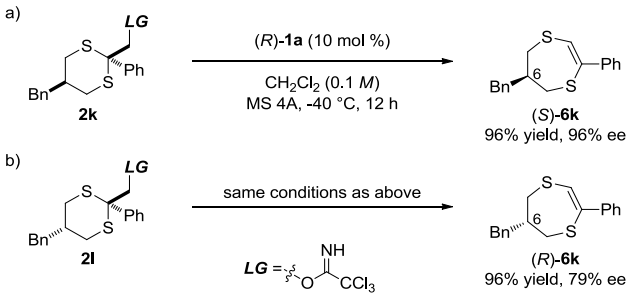

The reactions with *N*-methylpyrrole (**3c**) and *N*-methylindole (**3d**) were also carried out (Scheme 11). In these cases, ring expansion/addition products ***N*-Me-4a**[18] and ***N*-Me-7a** were obtained in 23% and 32% yields, respectively and ring expansion/deprotonation product **6a** was the major product. The ee values of ***N*-Me-4a** and ***N*-Me-7a** are not suitable for mechanistic discussion, because the existence of two competing reaction pathways would probably lead to the partial resolution of the enantio-enriched ("well-ordered") reactive intermediate under the influence of the chiral catalyst.[19]

Scheme 11. Reactions with *N*-methylpyrrole and *N*-methylindole.

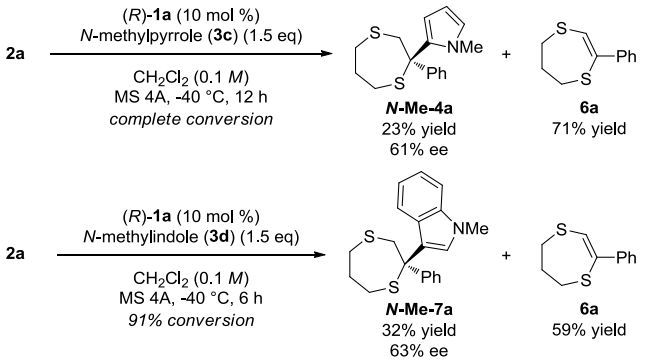

The yields of ring expansion/addition products ***N*-Me-4a** and ***N*-Me-7a** were low in the reactions with *N*-methylpyrrole (**3c**) and *N*-methylindole (**3d**), respectively (Scheme 11). In sharp contrast, pyrrole (**3a**) and indole (**3b**) underwent the ring expansion/addition reaction in excellent yields without the formation of ring expansion/deprotonation product **6** (Tables 1 and 2). These observations contradict the idea that, in principle, a more reactive nucleophile should give a ring expansion/addition product in higher yield, because **3c** and **3d** are more nucleophilic than **3a** and **3b**, respectively.[20] The results obtained using *N*-methyl derivatives **3c** and **3d** clearly reveal that the N-H moiety of **3a** and **3b** is the key to achieving high chemoselectivity. It is considered that the N-H moiety of these nucleophiles stabilizes the chiral phosphate anion generated throughout the ring expansion/addition process. The hydrogen bonding interaction between the N-H moiety and the oxygen atom of the phosphate anion is probably essential to circumvent the formation of ring expansion/deprotonation product **6** because of a decrease in basicity of the phosphate anion.

Possible structures of "well-ordered" reactive intermediate

From the experimental studies demonstrated above, we conclude that this reaction proceeds through an enantioselective 1,2-sulfur rearrangement/stereospecific nucleophilic addition sequence and a nucleophile, pyrrole or indole, is involved in the initial 1,2-sulfur rearrangement step.[21] However, the structure of the "well-ordered" reactive intermediate and the intrinsic nature of the stereospecific nucleophilic addition have remained unclear.

Three pathways are theoretically conceivable to fulfill the requirements of the stereospecific addition (Scheme 12).

[1] Path A: As the 1,2-sulfur rearrangement with the elimination of a leaving group is well recognized as an S_N2 process, episulfonium intermediate **INT-A** should be firstly generated. The product is formed from **INT-A** through S_N2-like transition state **TS-A**.

[2] Path B: Episulfonium intermediate **INT-A** undergoes ring opening to form **INT-B** immediately.[22] Meanwhile, thionium ion and phosphate anion maintain their relative positions in **INT-B**, namely, the formation of a "fixed" contact ion pair. Phosphate stays on one side of the thionium basal plane and does not change its original position to the other side. It is entirely different from the ion-pair structure presumed initially because the relative positions of thionium and phosphate are not restricted in the conventional assumption (Scheme 1b). Then, phosphate anion directs a nucleophilic attack from the same side on the thionium basal plane, affording the product through **TS-B** in a stereospecific manner.

[3] Path C: By directly transforming from **INT A** or through **INT-B**, the generation of covalently bonded phosphate intermediate **INT-C**[10c,23] is also considered possible by the addition of phosphate to episulfonium or thionium. Subsequent *syn* displacement of phosphate by the nucleophile from **INT-C** affords the product through concerted asynchronous transition state **TS-C**, namely, the S_Ni reaction pathway.[24]

Scheme 12. Possible intermediates and reaction pathways.

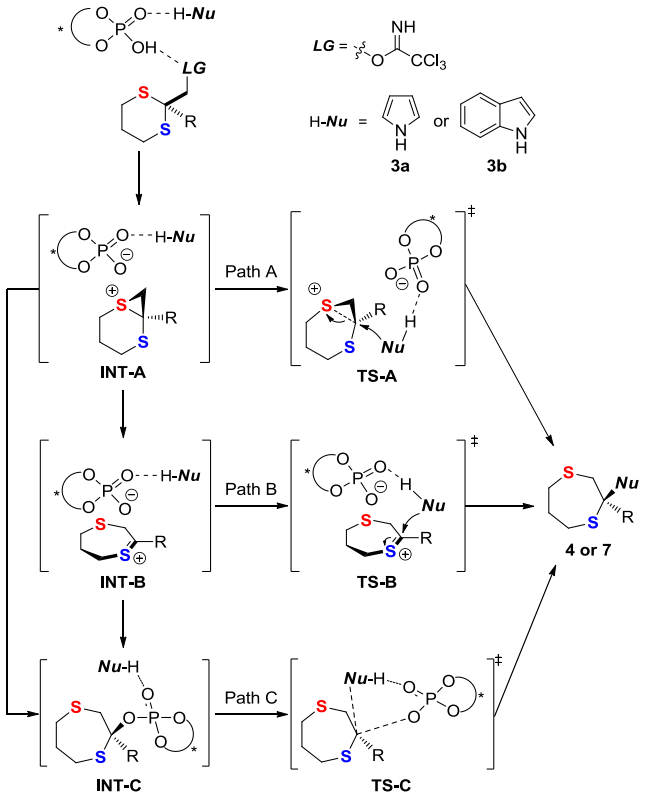

As mentioned in the previous section, the hydrogen bonding interaction between phosphate and nucleophile (H-***Nu***) shown in all the proposed intermediates not only decreases the basicity of phosphate but also increases the nucleophilicity of *N*-heterocyclic nucleophiles. Thus, the elimination is decelerated whereas the nucleophilic addition is accelerated.

To identify the structure of the "well-ordered" reactive intermediate, we performed NMR analyses and experimental studies by using achiral acid catalyst **1b** or other acid catalysts and changing the reaction solvents. At the outset, the reaction of **2a** with or without **3a** in the presence of **1b** (20 mol %) was monitored by ^{1}H and ^{31}P NMR spectroscopy (Figures S1 and S2). In the presence of **3a**, the gradual consumption of both reactants and the generation of ring expansion/addition product **4a** were observed and no other side products or intermediates, such as phosphate ester derivative **INT-C**, were detected by ^{1}H NMR measurement (Figure S1). Similarly, in the absence of **3a**, the ^{31}P NMR spectra displayed one slightly broad peak presumed to be phosphoric acid **1b** (Figure S2). No other phosphorus peaks were observed during the measurement, despite the fact that the phosphate anion would be one of the most nucleophilic species in the reaction system. We also conducted the reaction of **2k** and **2l** with **3a** using achiral acid catalysts with different acidities and in different solvents (Scheme 13: also see Tables S4–S6). The results indicate that high stereospecificity of the nucleophilic addition step is maintained in the reaction of **2k** even by changing the acidity of the catalyst and the polarity of the solvent employed, whereas in the reaction of **2l** the stereospecificity is highly dependent on these parameters. The reaction of **2l** using trifluoroacetic acid (TFA) (p*K*a 3.37 in DMSO),[25] of which acidity is slightly higher than that of phosphoric acid **1b** (p*K*a 3.72 in DMSO),[25] resulted in a decrease in stereospecificity to afford a diastereomeric mixture of **4k** and **4l** in 7:93 (Scheme 13a). The reduction of stereospecificity was also observed in the reaction of **2l** using **1b** in polar acetonitrile, instead of less polar dichloromethane, affording **4k** and **4l** in 10:90 (Scheme 13b). Enhancement of the catalyst acidity and the solvent polarity resulted in the reduction of stereospecificity in the reaction of **2l**.

Scheme 13. Effects of acids and solvents.

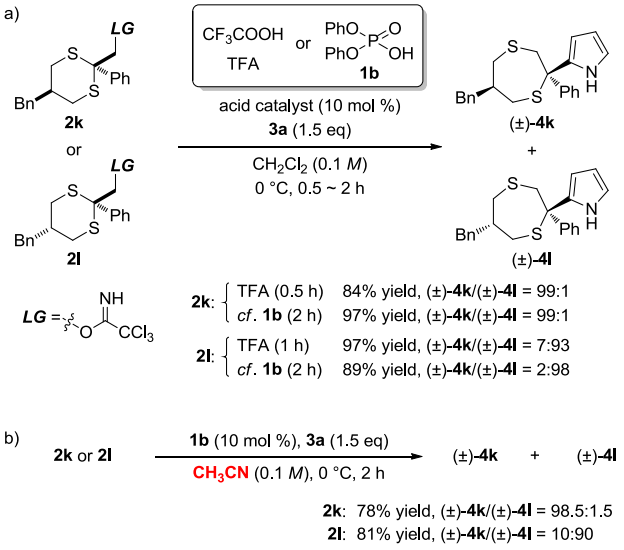

It should be pointed out that the reaction of **2k** proceeded in a stereospecific manner even by changing the acid catalyst and the solvent used. These results suggest that these parameters do not significantly affect the reaction mechanism when using **2k** as the substrate. It would be postulated that the reaction mechanism is maintained even by using **2l**, instead of **2k**, under these reaction conditions. On the basis of this postulation, Path A is unlikely because S_N2-like transition state **TS-A** is the origin of the stereospecificity in Path A, which is initiated from stereochemically well-defined episulfonium intermediate **INT-A**. Even if the catalyst acidity and the solvent polarity were changed, the stereospecificity originated from this assumed mechanism should be preserved in Path A. However, this is not consistent with the experimental observations in the reactions of **2l**. Furthermore, the experimental results, coupled with the NMR monitoring data, imply that Path C is also unlikely on the basis of the above postulation. In Path C, in principle, the stereospecificity is presumably preserved even by changing the reaction conditions because it would originate from the S_Ni reaction of stereochemically defined intermediate **INT-C** *via* transition state **TS-C**. **INT-C** would be generated from phosphate and episulfonium or thionium through the formation of a configurationally stable covalent bond that should aid the stereospecific process. However, the decrease in stereospecificity was observed in the reactions of **2l**. In addition, intermediate **INT-C** could not be observed clearly throughout the NMR monitoring process. Therefore, Path C is

probably not the plausible pathway, although the concerted S_Ni reaction is mechanistically intriguing.[24]

Based on the above considerations, the "fixed" contact ion pair of ring-expanded thionium ion and phosphate anion is the best candidate for the "well-ordered" reactive intermediate (Scheme 12, **INT-B**) and hence Path B is the plausible pathway for the stereospecific addition process. However, experimental evidence is not sufficient to completely rule out other possible pathways. Therefore, we further conducted DFT calculation to understand the reaction mechanism and identify the "well-ordered" reactive intermediate and the stereospecific reaction pathway.

DFT Calculation: model study

To simplify the calculation, phosphoric acid **1c** having a biphenol backbone as well as standard substrate **2a** and pyrrole (**3a**) were used in the model study (Scheme 14).[17,21,26] All calculations were performed with the Gaussian 09 package (Revision C.01).[27] Geometries were optimized and characterized using frequency calculations at the B97D/6-31G(d,p) level, unless otherwise noted.[28,29] Energies in the solution phase were calculated using single-point energy calculations at the same level according to the CPCM solvation model for the optimized structures.[30]

As **1c** has an axially chiral structure [(*R*)-isomer], the generation of major enantiomer (*R*)-**4a** was calculated as observed in the experimental results. From the mechanistic studies shown above, we added pyrrole in the calculation from the initial 1,2-sulfur rearrangement step even for the model studies.

Scheme 14. Model system for calculation.

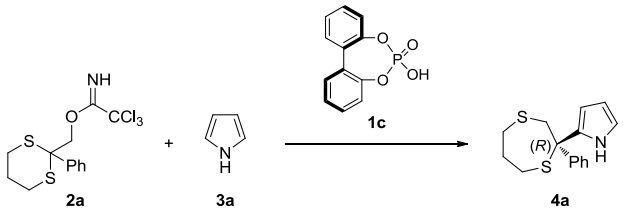

The reaction is known to be initiated by a nucleophilic attack by one of the sulfur atoms of 1,3-dithiane and the elimination of the leaving group *via* the S_N2 mechanism.[7,31] In calculating the transition states of this initial step, the orientation of the leaving group and the location of phosphoric acid catalyst were carefully considered. The trichloroacetimidate group would adopt an axial or equatorial orientation. In the meantime, phosphoric acid would locate in the proximity of 1,3-dithiane or far from it. Considering various combinations of these orientations, four possible transition states were calculated.[32] As shown in Figure 2a, **TS-1-axial-in**, in which the leaving group is located at the axial position and phosphoric acid is close to 1,3-dithiane, turned out to be the most favorable transition state. In contrast, **TS-1-axial-out** is energetically disfavored even though the steric congestion between phosphate and 1,3-dithiane is avoided. More interestingly, as observed in **TS-1-equatorial-in** and **TS-1-equatorial-out**, the optimization of transient structures, which was performed from the initial structures having the leaving group at the equatorial position, enforced a conformational change in 1,3-dithiane from the chair form to the boat-like one with the leaving group occupying the axial position (Figure 2a). These results clearly indicate that the axial orientation of the leaving group is much more favorable for the nucleophilic attack by sulfur atom than the equatorial one, although these conformational changes eventually lead to the destabilization of these transition states.

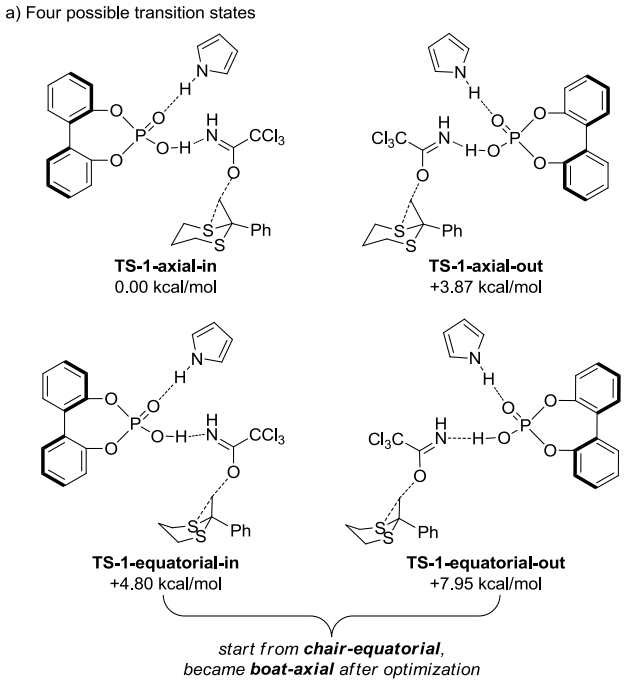

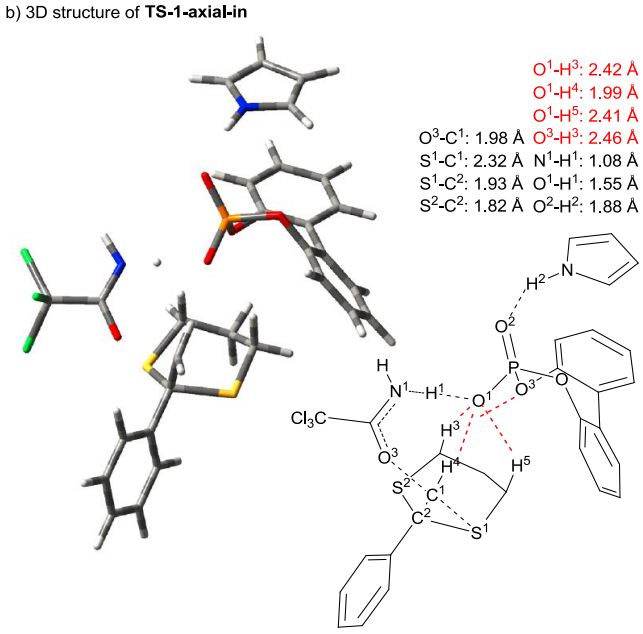

Figure 2. Transition states for sulfur rearrangement. Geometries were optimized and characterized using frequency calculations at the B97D/6-31G(d,p) level. Relative free energies (kcal/mol) obtained by single-point energy calculations at the same level for the optimized structures with the SCRF method based on CPCM (ϵ = 8.93 for CH_2Cl_2) are shown.

The 3D structure of energetically most favorable **TS-1-axial-in** is shown in Figure 2b. Phosphoric acid **1c** protonates the nitrogen atom of the leaving group to form a hydrogen bond and pyrrole also forms a hydrogen bond with phosphoryl oxygen. More importantly, four non-classical C-H···O hydrogen bonds are also clearly observed between 1,3-dithiane and

phosphate anion. These C-H···O hydrogen bonds, namely, electrostatic interaction,[3,33,34] stabilize the transition structures of partially generated phosphate anion, the location of which is regulated in proximity to 1,3-dithiane by these interactions. This orientation results in the efficient reduction of the degree of charge separation in this transition state, albeit causing steric congestion between these partially charged moieties.

Based on the calculations shown in Figure 2, the difference in reactivity between substrates **2k** and **2l** is well rationalized (Scheme 15). The experimental results revealed that **2k** was more reactive than **2l** (Scheme 2, condition 1: 100% conversion of **2k**, 56% conversion of **2l**). As shown in Figure 2a, the sulfur rearrangement is more favorable for the leaving group located at the axial position than for that located at the equatorial position. **2k-ax** and **2l-ax** should be the reactive conformers for **2k** and **2l**, respectively (Scheme 15). However, **2k-ax** and **2l-eq** were the favored conformers on the basis of the ^{1}H NMR analysis of **2k** and **2l**, respectively, involving NOE experiments (based on coupling constants and NOE, see NMR spectra of **2k** and **2l** in SI for details). A conformational change is required of **2l** from thermodynamically stable **2l-eq** to less stable **2l-ax**, because the axial orientation of the leaving group is necessary for the sulfur rearrangement. In contrast, no conformational change is necessary for thermodynamically favorable **2k-eq** and hence **2k** exhibits higher reactivity than **2l**. It is therefore considered that the sulfur rearrangement would be the rate-determining step (RDS) of the overall reaction. The results of NMR monitoring showed that no other species were observed except the starting material, the catalyst, and the product (Figures S1 and S2) also suggests that the initial sulfur rearrangement is RDS.[17] In order to confirm whether the sulfur rearrangement is RDS or not and to further elucidate the "well-ordered" reactive intermediate, we clarified the energy profile of this reaction.

Scheme 15. Possible reason for the difference in reactivity between 2k and 2l.

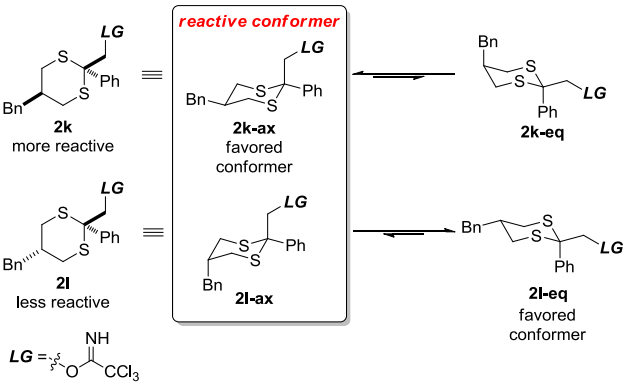

The energy profile is shown in Figure 3. The largest energy barrier is the initial step, namely, the 1,2-sulfur rearrangement with elimination of the leaving group (**TS-1-axial-in**), and hence this step is indeed RDS. After this transition state, in principle, the episulfonium ion should be formed as the proximate intermediate. However, subsequent analysis of the intrinsic reaction coordinate (IRC) from **TS-1-axial-in** revealed the formation of ion-pair intermediate **INT-1** consisting of ring-expanded thionium ion, phosphate anion, and trichloroacetamide as the next meta-stable intermediate. The IRC analysis clearly indicates that episulfonium undergoes ring opening immediately, even if episulfonium would form with a small energy barrier, and thus it should not be the intermediate for the nucleophilic addition (Scheme 12: Path A is ruled out). A clue for the immediate ring expansion is also obtained from the bond length data of **TS-1-axial-in** (Figure 2b). The S^1-C^2 bond elongates to 1.93 Å, thus becoming weaker, whereas the S^2-C^2 bond measures 1.82 Å, which is in the normal range of a S-C single bond.[35]

From **INT-1**, after trichloroacetamide is cleaved off, more stable contact ion-pair intermediate **INT-2** is generated and is consistent with **INT-B** (Scheme 12). Followed by a small energy barrier, 4.3 kcal/mol, nucleophilic addition takes place smoothly to afford C-C bond formation intermediate **INT-4** *via* **TS-2**. After a proton shift to aromatize, addition product **4a** complexed with **1c** is formed. The formation of a C-O bond from **INT-2** affords covalent bonded phosphate **INT-3**, consistent with **INT-C** (Scheme 12), and **INT-3** is energetically disfavored compared to **INT-2**. The energy level of **INT-3** is comparable to that of **TS-2**. Even when pyrrole is removed, adduct **INT-3'** is still less stable than **INT-2**. This indicates that phosphate adducts **INT-3'** and **INT-3** should not be the reactive intermediate in this reaction (Scheme 12: Path C is ruled out).

The energy profile of the overall processes clearly reveals that the ion pair of ring-expanded thionium and phosphate **INT-2** (= **INT-B**) can be regarded as the "well-ordered" reactive intermediate. In order to understand how and why the stereospecific addition proceeded *via* this intermediate, we carefully analyzed the 3D structures of **INT-2** and the transition state of nucleophilic addition, **TS-2**. As shown in Figure 4a, in **INT-2**, five C-H···O hydrogen bonds are formed between thionium and phosphate, similar to that observed in **TS-1-axial-in** (Figure 2b). In addition, phosphate directs pyrrole to locate in close proximity through the O···H···N hydrogen bond and hence phosphate as well as pyrrole is localized on the same side of the thionium framework.

The structure of **TS-2** (Figure 4b) is apparently the same as that of **INT-2** (Figure 4a) except for the slight variation of the relative positions between these ternary fragments. Most of the key interactions in **INT-2** are observed in **TS-2** with a minor change of the interaction pattern of the multiple C-H···O hydrogen bonds between thionium and phosphate. Besides these hydrogen bonding interactions, σ-hyperconjugation, $\sigma^*(S^1\text{-}C)$-$\sigma(C\text{-}C)_{formation}$, should also be taken into consideration. **TS-2** is stereo-electronically preferred for the nucleophilic attack on thionium, because the forming C-C bond is stabilized by the antiperiplanar effect of the S^1-C bond (Figure 4b).[36]

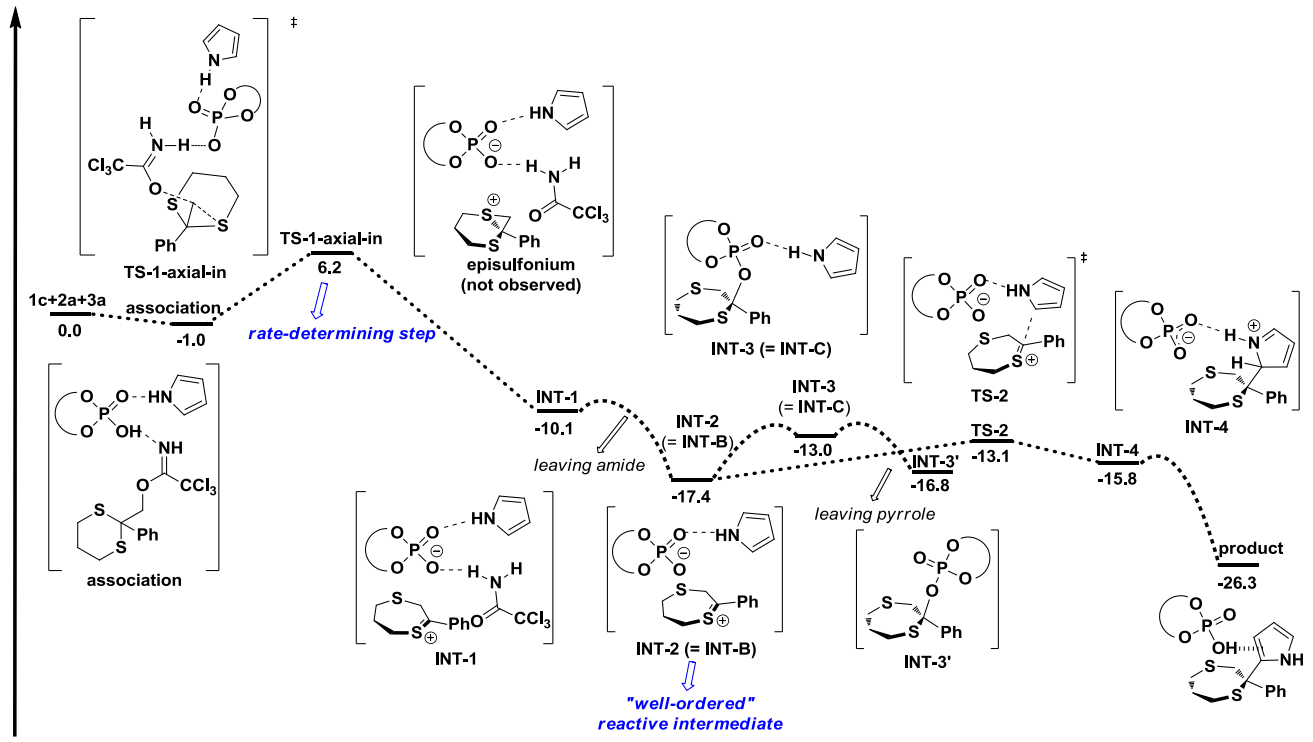

Figure 3. Energy profile of model reaction. The potential energy for the sum of **1c**, **2a**, and **3a** was set to zero. Geometries were optimized and characterized using frequency calculations at the B97D/6-31G(d,p) level. Energies (kcal/mol) in solution phase were calculated using single-point energy calculations at the same level for the optimized structures according to the SCRF method based on CPCM (CH_2Cl_2).

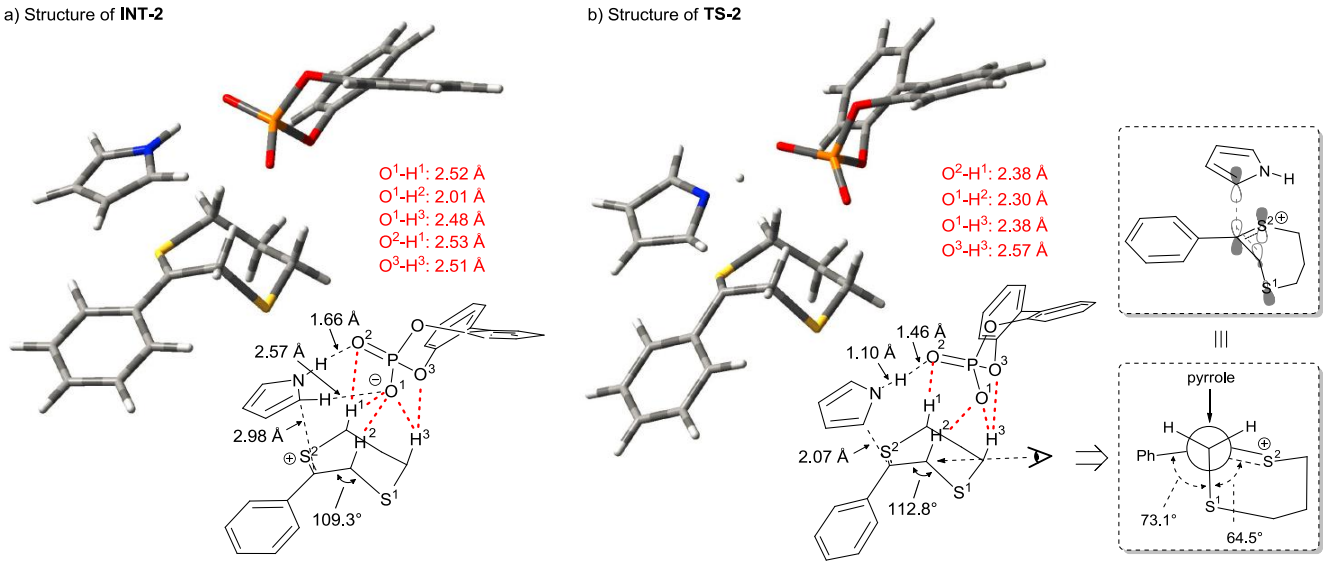

Figure 4. 3D models of **INT-2** and **TS-2**.

Three factors: (i) C-H···O hydrogen bonds between thionium and phosphate, (ii) phosphate anion directing nucleophile through a hydrogen bond, and (iii) σ-hyperconjugation, participate synergistically to establish this highly stereospecific addition process. As regards the origin of this stereospecific addition, it should result from the location of the phosphoric acid catalyst in the 1,2-sulfur rearrangement. This is because C-H···O hydrogen bonds are formed between phosphoric acid **1** and 1,3-dithiane substrate **2** in **TS-1-axial-in**, the transition state of the sulfur rearrangement, in which phosphoric acid is in proximity to 1,3-dithiane on the same side of the axially oriented leaving group (Figure 2b). Phosphoric acid/phosphate and 1,3-dithiane/thionium are tethered by the C-H···O hydrogen bonds from the initial sulfur rearrangement step and hence the relative positions of these fragments do not change from the 1,2-sulfur rearrangement, ring expansion, and elimination

of the leaving group steps to the nucleophilic addition step. It can be concluded that the ternary association of phosphoric acid, substrate, and nucleophile through the C-H···O and N···H···O hydrogen bonds is the origin not only of the "well-ordered" reactive intermediate but also of the stereospecific addition.[37]

As the ternary association in the initial sulfur rearrangement step is the origin of the stereospecific addition, it is surmised that the use of (*E*)-*N*-phenyltrifluoroacetimidate as the leaving group would also allow the reaction to proceed in a stereospecific manner (Figure 5). That is because the (*E*)-geometry of the *N*-phenyl group should form a transient structure similar to that observed in the substrate having the trichloroacetimidate group, albeit resulting in low reactivity and enantioselectivity as expected from Scheme 3.

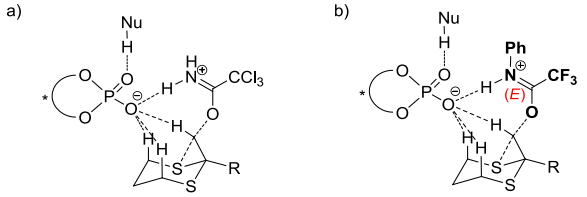

Figure 5. Proposed transition states of 1,2-sulfur rearrangement of substrates with different leaving groups.

With this hypothesis in mind, the reaction of dithiane **5l** having (*E*)-*N*-phenyltrifluoroacetimidate with pyrrole **3a** (1.5 equiv.) was conducted using 10 mol % of optimized catalyst (*R*)-**1a** and MS 4A in dichloromethane at room temperature for 4 h (Scheme 16a).[16] Substrate conversion was only 34% and desired product (2*S*,6*S*)-**4l** was obtained in 25% NMR yield with 98:2 dr and 15% ee. In comparison with **5l**, the reaction of **2l** under the same conditions proceeded smoothly and complete conversion was achieved within 1 h (Scheme 16b). Product (2*R*,6*R*)-**4l** was obtained in 81% NMR yield with 99:1 dr and 51% ee. In both cases, ring expansion/deprotonation product (*R*)-**6k** was obtained as the by-product. These results verify our hypothesis that the reaction using (*E*)-*N*-phenyltrifluoroacetimidate as the leaving group is also stereospecific, although the reactivity was much lower than that of the substrate having the trichloroacetimidate group. Once again, the different enantioselectivities of these two reactions clearly reveal that EDS should be the 1,2-sulfur rearrangement instead of the following nucleophilic addition (Scheme 9).

Scheme 16. Stereospecificity of reactions using substrates with different leaving groups.

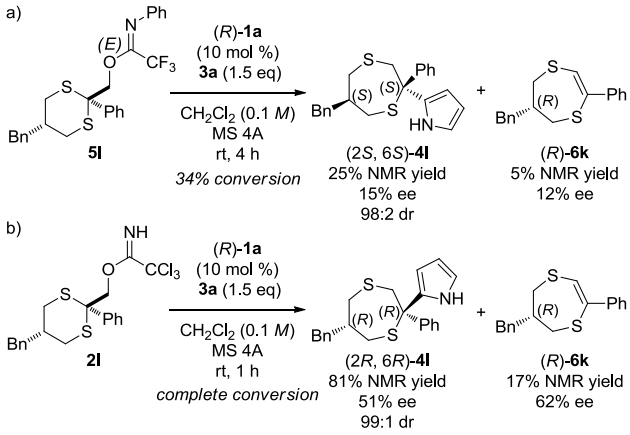

DFT calculation of enantio-determining step (EDS): Real system

The reaction pathway and the reactive intermediate were clarified on the basis of experimental studies and model calculations. We next turned our attention to elucidation of the mechanism underlying EDS, in particular, the intriguing substituent effect at the 5-position of 1,3-dithiane. The substituent at the 5-position *cis* to the leaving group of 1,3-dithiane substrate **2k** enhances the enantioselectivity markedly, as compared with **2l** having a substituent *trans* to the leaving group (Table 1 and Scheme 2). In order to gain an insight into the origin of the stereochemical outcome as well as the substituent effect at the 5-position of 1,3-dithiane, we calculated EDS, namely, the 1,2-sulfur rearrangement step, using substrate **2k** and catalyst (*R*)-**1a** instead of simplified acid catalyst **1c**. To expedite our calculation, no nucleophile is added because based on our experimental result with or without using pyrrole as the nucleophile, the enantioselectivity of ring-expansion/addition product **4k** is identical to that of ring-expansion/deprotonation product (*S*)-**6k** (Schemes 2a and 10a). This implies that the structures of these transition states are fundamentally similar in EDS, irrespective of the presence or absence of pyrrole.

The computed transition states for both major and minor reaction pathways of the reaction using **2k** are shown in Figure 6. The energy difference between these two transition states is 2.6 kcal/mol with the one resulting in (*S*)-**6k** being the energetically favored one. The result of the calculations is consistent with the experimental finding that (*S*)-**6k** is the major enantiomer in the reaction of **2k** catalyzed by (*R*)-**1a** (Scheme 10), although the expected enantiomeric excess calculated from the energy difference does not perfectly match the experimental result.[38]

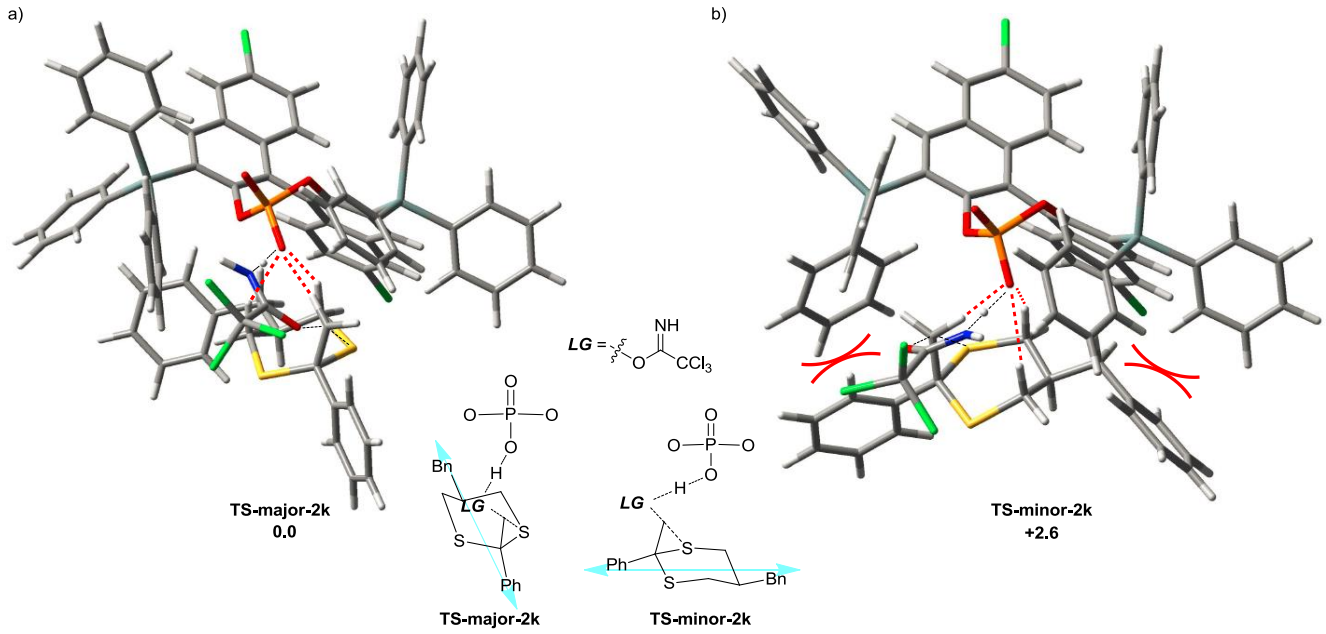

Figure 6. Transition states of EDS of **2k** with catalyst (*R*)-**1a**. Geometries were optimized and characterized using frequency calculations at the B97D/6-31G(d,p) level. Relative free energies (kcal/mol) obtained by single-point energy calculations at the same level for the optimized structures with the SCRF method based on CPCM (CH_2Cl_2) are shown.

By carefully analyzing the key interactions in these two transition states, three non-classical C-H···O hydrogen bonds were observed in not only **TS-major-2k** but also **TS-minor-2k**. This indicates that these C-H···O hydrogen bonds formed between the substrate and the catalyst are vital to determine the relative positions accurately and hence these interactions are the key to differentiating the major and minor pathways. In fact, the relative arrangements of **2k** and (*R*)-**1a** are absolutely different in these two transition states. In **TS-minor-2k**, **2k** is oriented from side to side as shown in Figure 6b, where the phenyl group is located close to one of the bulky triphenylsilyl groups, resulting in steric repulsion. In addition, the steric congestion between the benzyl group introduced at the 5-position and the other triphenylsilyl group further destabilizes this transition state. In contrast, in **TS-major-2k** (Figure 6a), substrate **2k** is placed back and forth to avoid steric congestion between the two triphenylsilyl groups and the phenyl group substituted at the 2-position. Furthermore, the benzyl group introduced at the 5-position is oriented in such a way as to avoid steric repulsion with the triphenylsilyl group and further stabilize this transition state through the T-shape C-H···π interaction[39,40] with the phenyl ring of the triphenylsilyl group. The substituent effect at the 5-position of 1,3-dithiane is also well rationalized based on these transition structures. In the substrates having the substituent *cis* to the leaving group, namely, **2k** as well as **2i** and **2j**, the substituent occupies the equatorial position of 1,3-dithiane to induce repulsive interaction with the triphenylsilyl group in the minor transition state, as likely shown in Figure 6b, resulting in a marked increase in enantioselectivity (Table 1). In contrast, in the reaction of **2l** having a substituent *trans* to the leaving group, steric congestion does not occur between the triphenylsilyl group and the substituent in the minor transition state, because the substituent is located in the axial position and exhibits little effect on the enantioselectivity.

CONCLUSION

We have reported herein our in-depth mechanistic case study of a newly developed CPA-catalyzed enantioselective ring expansion reaction of 1,3-dithiane derivatives. Experimental studies were well-designed to elucidate that an unprecedented enantioselective 1,2-sulfur rearrangement/stereospecific nucleophilic addition sequence is the concrete mechanism. This discovery is completely different from conventionally assumed two-step reactions. Moreover, a nucleophile is involved not only in the nucleophilic addition step, but also in the initial 1,2-sulfur rearrangement step, even though it does not directly react with the substrate in the initial step.

The structure of the "well-ordered" reactive intermediate and the intrinsic nature of the stereospecific nucleophilic addition were identified by DFT calculation using a simplified model, where non-classical C-H···O hydrogen bonds formed between the phosphoric acid catalyst and the substrate were found to be the key interaction in this reaction. These hydrogen bonds not only linked the catalyst with the substrate to form energetically favored states, but also firmly maintained their relative positions and stored chiral information as the "fixed" contact ion pair in the reactive intermediates during the overall processes.

The origin of the enantio-control by CPA was also elucidated by DFT calculation of the real reaction system. In EDS, non-classical C-H···O hydrogen bonds were involved in the key interaction. Moreover, it was confirmed that the intriguing substituent effect at the 5-position of 1,3-dithiane originated from the interaction between the substituent at the 5-position

cis to the leaving group and the triphenylsilyl groups at the 3,3'-positions of CPA.

This mechanistic case study provided a very clear understanding of the nature of the ion-pairing interaction in CPA-catalyzed reactions. It will be very helpful for the further development of novel organocatalytic transformations using a CPA catalyst. The results of this in-depth mechanistic case study are expected to hasten the design of new organocatalysts in the future.

ASSOCIATED CONTENT

Supporting Information.

The exploratory investigation, experimental procedures and characterization data. This material is available free of charge via the Internet at http://pubs.acs.org.

AUTHOR INFORMATION

Corresponding Author

mterada@m.tohoku.ac.jp

Notes

The authors declare no competing financial interest.

Present Address

†F.L.: Department of Chemical and Environmental Engineering, Yale University, New Haven, CT 06511, USA.

Author Contributions

All authors have given approval to the final version of the manuscript.

ACKNOWLEDGMENT

This work was partially supported by a Grant-in-Aid for Scientific Research on Innovative Areas "Advanced Molecular Transformations by Organocatalysts" from The MEXT, Japan (No. 23105002). We thank JSPS for a research fellowship for Young Scientists (F.L.).

ABBREVIATIONS

CPA, chiral phosphoric acid; EDS, enantio-determining step; IRC, intrinsic reaction coordinate; NOE, nuclear Overhauser effect; RDS, rate-determining step.

REFERENCES

(1) For selected reviews about chiral anion controlled asymmetric catalysis, see: (a) Lacour, J.; Moraleda, D. *Chem. Commun.* **2009**, 7073-7089. (b) Phipps, R. J.; Hamilton, G. L.; Toste, F. D. *Nat. Chem.* **2012**, *4*, 603-614. (c) Parra, A.; Reboredo, S.; Castro, A. M. M.; Alemán, J. *Org. Biomol. Chem.* **2012**, *10*, 5001-5020. (d) Mahlau, M.; List, B. *Angew. Chem., Int. Ed.* **2013**, *52*, 518-533. (e) Brak, K.; Jacobsen, E. N. *Angew. Chem., Int. Ed.* **2013**, *52*, 534-561. Also see: (f) Parmar, D.; Sugiono, E.; Raja, S.; Rueping, M. *Chem. Rev.* **2014**, *114*, 9047-9153.

(2) Seminal works of chiral phosphoric acid, see: (a) Akiyama, T.; Itoh, J.; Yokota, K.; Fuchibe, K. *Angew. Chem., Int. Ed.* **2004**, *43*, 1566-1568. (b) Uraguchi, D.; Terada, M. *J. Am. Chem. Soc.* **2004**, *126*, 5356-5357. For selected reviews of chiral phosphoric acid, see: (c) Akiyama, T. *Chem. Rev.* **2007**, *107*, 5744-5758. (d) Adair, G.; Mukherjee, S.; List, B. *Aldrichimica Acta* **2008**, *41*, 31-39. (e) Terada, M. *Chem. Commun.* **2008**, 4097-4112. (f) Terada, M. *Synthesis* **2010**, 1929-1982. Also see: Ref. 1f.

(3) Kanomata, K.; Toda, Y.; Shibata, Y.; Yamanaka, M.; Tsuzuki, S.; Gridnev, I. D.; Terada, M. *Chem. Sci.* **2014**, *5*, 3515-3523.

(4) Selected recent reviews of thionium mediated reactions, see: (a) Bur, S. K.; Padwa, A. *Chem. Rev.* **2004**, *104*, 2401-2432. (b) Feldman, K. S. *Tetrahedron* **2006**, *62*, 5003-5034. (c) Smith, L. H. S.; Coote, S. C.; Sneddon, H. F.; Procter, D. J. *Angew. Chem., Int. Ed.* **2010**, *49*, 5832-5844.

(5) Examples of chiral anion controlled asymmetric catalysis using another sulfur-stabilized carbocations, see: (a) Hamilton, G. L.; Kanai, T.; Toste, F. D. *J. Am. Chem. Soc.* **2008**, *130*, 14984-14986. (b) Lin, S.; Jacobsen, E. N. *Nat. Chem.* **2012**, *4*, 817-824.

(6) Recent comprehensive review of asymmetric catalytic synthesis of optically active sulfur compounds having quaternary stereogenic center, see: Yu, J.-S.; Huang, H.-M.; Ding, P.-G.; Hu, X.-S.; Zhou, F.; Zhou, J. *ACS Catal*. **2016**, *6*, 5319-5344.

(7) For selected reviews of 1,2-sulfur rearrangement, see: (a) Fox, D. J.; House, D.; Warren, S. *Angew. Chem., Int. Ed*. **2002**, 41, 2462-2482. (b) Sromek, A. W.; Gevorgyan, V. *Top. Curr. Chem.* **2007**, *274*, 77-124. For selective papers of 1,2-sulfur rearrangement, see: (c) Marshall, J. A.; Roebke, H. *J. Org. Chem.* **1969**, *34*, 4188-4191. (d) Gateau-Olesker, A.; Sepulchre, A. M.; Vass, G.; Géro, S. D. *Tetrahedron* **1977**, *33*, 393-397. (e) Tarnchompoo, B.; Thebtaranonth, Y. *Tetrahedron Lett*. **1984**, *25*, 5567-5570. (f) Nickon, A.; Rodriguez, A. D.; Shirhatti, V.; Ganguly, R. *J. Org. Chem.* **1985**, *50*, 4218-4226. (g) Saigo, K.; Hashimoto, Y.; Fang, L.; Hasegawa, M. *Heterocycles* **1989**, *29*, 2079-2082. (h) Afonso, C. A. M.; Barros, M. T.; Godinho, L. S.; Maycock, C. D. *Synthesis* **1991**, 575-580. (i) Barros, M. T.; Maycock, C. D.; Santos, L. S. *Heterocycles* **1998**, *48*, 1121-1138. (j) Afonso, C. A. M.; Barros, M. T.; Maycock, C. D. *Tetrahedron* **1999**, *55*, 801-814. (k) Michel, K.; Glotzbach, C.; Fröhlich, R.; Würthwein, E.-U. *Eur. J. Org. Chem.* **2012**, 960-966.

(8) See Supporting Information (Table S1 and S2) for details.

(9) 1,3-dithiolane (five-membered ring) and 1,3-dithiepane derivatives (seven-membered ring) were also employed as the substrate under the optimized reaction conditions [(*R*)-**1a** (10 mol%) in CH_2Cl_2 at -40 ºC for 12 h]. The reactions of these cyclicdithioacetals having the phenyl substituent with pyrrole (**3a**) afforded the corresponding 1,4-dithiane product **4m** and 1,4-dithiocane product **4n** in 75% yield with 32% ee and in 79% yield with 64% ee, respectively. See SI for details.

(10) For examples of using BINOL-derived chiral phosphoric acid with electron-withdrawing group at 6,6'-position, see: (a) Akiyama, T.; Honma, Y.; Itoh, J.; Fuchibe, K. *Adv. Synth. Catal*. **2008**, *350*, 399-402. (b) Harada, S.; Kuwano, S.; Yamaoka, Y.; Yamada, K.; Takasu, K. *Angew. Chem., Int. Ed.* **2013**, *52*, 10227-10230. (c) Kuroda, Y.; Harada, S.; Oonishi, A.; Kiyama, H.; Yamaoka, Y.; Yamada, K.; Takasu, K. *Angew. Chem., Int. Ed.* **2016**, *55*, 13137-13141.

(11) The attempt to synthesize a substrate bearing an electron-donating 4-methoxyphenyl group failed.

(12) Supplementary crystallographic data of **4f**, **4k**, **2l** and **5d** are deposited at the Cambridge Crystallographic Data Center. The deposition numbers of them are CCDC 1437351 (**4f**), CCDC 1437411 (**4k**), CCDC 1520496 (**2l**), and CCDC 1520496 (**5d**), respectively.

(13) The geometries of **2k** and **2l** were determined by NMR analysis in combination with NOE spectra and coupling constants J_{HH} (See SI for details). The geometry of **2l** was also determined by single-crystal X-ray crystallography.

(14) The absolute stereochemistries of **4l**, **6k**, **7k**, and **7l** were unambiguously determined by chemical derivatizations on the basis of the stereochemically assigned (2*R*,6*S*)-**4k** whose stereochemistry has been determined by X-ray crystallography. See SI for details.

(15) The geometry of the C=N double bond of **5d** was determined to be *E* by X-ray crystallography. However, *N*-aryl imidates were reported to undergo facile *E/Z* isomerization based on the line broadening phenomenon of the *N*-aryl moiety in the NMR spectrum, see: Fischer, D. F.; Barakat, A.; Xin, Z.-Q.; Weiss, M. E.; Peters, R. *Chem. Eur. J.* **2009**, *15*, 8722-8741. We did not observe such line broadening in the NMR spectra of **5d** and **5l**.

(16) When the reaction of **5** was conducted under the optimized conditions (-40 ºC, 12 h), no conversion of **5** was observed.

(17) Kinetic studies were carried out by changing the concentration of pyrrole (**3a**) (0.10, 0.15, 0.30, and 0.60 *M*) under the optimized

reaction conditions (using 10 mol% (*R*)-**1a** and 0.10 *M* solution of **2a** in CH_2Cl_2 at -40 °C). As the result, the rate of the reaction was dependent on the concentration of pyrrole (**3a**), however it was reduced when increasing the concentration of **3a**. Thus, **3a** was found to function as an inhibitor of the present reaction and hence it is difficult to conclude whether **3a** is involved into the rate-determining step or not on the basis of the present kinetic studies. See SI for details.

(18) The absolute configuration of the major enantiomer of ***N*-Me-4a** was determined to be *R* by derivatization (See SI for details). This selectivity is probably explained by using the following model:

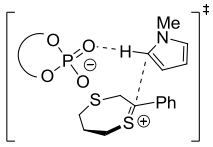

TS-*N*-Me-4a

This C_{Nu}-H···O hydrogen bond has been reported in the CPA-catalyzed enantioselective Friedel-Crafts reaction of 2-methoxyfuran with ketimine, see: Kondoh, A.; Ota, Y.; Komuro, T.; Egawa, F.; Kanomata, K.; Terada, M. *Chem. Sci.* **2016**, *7*, 1057-1062.

(19) The reactions of **2l** with *N*-methylpyrrole (**3c**) and *N*-methylindole (**3d**) were also carried out under the optimized reaction conditions. In both of the reactions, the ring expansion/deprotonation product (*R*)-**6k** was obtained as the major product in 88% yield with 82% ee for **3c** and in 81% yield with 81% ee for **3d**. The ring expansion/addition products ***N*-Me-4l** (derived from **3c**) and ***N*-Me-7l** (derived from **3d**) were obtained in a nearly diastereomerically pure form (***N*-Me-4l**: 11% yield, 98.5:1.5 dr, 76% ee, ***N*-Me-7l**: 19% yield, >99:1 dr, 72% ee) and hence the reaction proceeded in a stereospecific manner, regardless in the absence/presence of the hydrogen bond donor nucleophile. In addition, the observed ee values of ***N*-Me-4l** and ***N*-Me-7l** were slightly lower than those of (*R*)-**6k**. These results suggest that parallel kinetic resolution of the enantio-enriched ("well-ordered") reactive intermediate occurred under the influence of the chiral phosphate anion.

(20) (a) Mayr, H.; Bug, T.; Gotta, M. F.; Hering, N.; Irrgang, B.; Janker, B.; Kempf, B.; Loos, R.; Ofial, A. R.; Remennikov, G.; Schimmel, H. *J. Am. Chem. Soc.* **2001**, *123*, 9500-9512. (b) Kempf, B.; Hampel, N.; Ofial, A. R.; Mayr, H. *Chem. Eur. J.* **2003**, *9*, 2209-2218. (c) Lakhdar, S.; Westermaier, M.; Terrier, F.; Goumont, R.; Boubaker, T.; Ofial, A. R.; Mayr, H. *J. Org. Chem.* **2006**, *71*, 9088-9095.

(21) The kinetic studies were performed to determine the reaction order and it was confirmed that the reaction is first order in the catalyst. Therefore the monomeric catalyst was considered to be involved in the system. See SI for details.

(22) For a review of the reactive intermediate, episulfonium ions and oxocarbenium ions, see: Beaver, M. G.; Billings, S. B.; Woerpel, K. A. *Eur. J. Org. Chem.* **2008**, 771-781.

(23) Covalent bonded phosphate intermediate has been proposed in some chiral phosphoric acid catalyzed reactions, see: (a) Sun, Z.; Winschel, G. A.; Zimmerman, P. M.; Nagorny, P. *Angew. Chem., Int. Ed.* **2014**, *53*, 11194-11198. (b) Liu, L.; Leutzsch, M.; Zheng, Y.; Wasim Alachraf, M.; Thiel, W.; List, B. *J. Am. Chem. Soc.* **2015**, *137*, 13268-13271. (c) Khomutnyk, Y. Y.; Argüelles, A. J.; Winschel, G. A.; Sun, Z.; Zimmerman, P. M.; Nagorny, P. *J. Am. Chem. Soc.* **2016**, *138*, 444-456. (d) Tay, J.-H.; Argüelles, A. J.; DeMars II, M. D.; Zimmerman, P. M.; Sherman, D. H.; Nagorny, P. *J. Am. Chem. Soc.* **2017**, *139*, 8570-8578.

(24) For selected examples of mechanistic studies of S_Ni reaction, see: (a) Sinnott, M. L.; Jencks, W. P. *J. Am. Chem. Soc.* **1980**, *102*, 2026-2032. (b) Guthrie, R. D.; Jencks, W. P. *Acc. Chem. Res.* **1989**, *22*, 343-349. (c) Lee, S. S.; Hong, S. Y.; Errey, J. C.; Izumi, A.; Davies, G. J.; Davis, B. G. *Nature Chem. Biol.* **2011**, *7*, 631-638. (d) Chan, J.; Tang, A.; Bennet, A. J. *J. Am. Chem. Soc.* **2012**, *134*, 1212-1220. (e) Blanco Capurro, J. I.; Hopkins, C. W.; Pierdominici Sottile, G.; González Lebrero, M. C.; Roitberg, A. E.; Marti, M. A. *J. Phys. Chem. B* **2017**, *121*, 471-478.

(25) Christ, P.; Lindsay, A. G.; Vormittag, Sonja S.; Neudcrfl, J.-M.; Berkessel, A.; O'Donoghue, A. C. *Chem. Eur. J.* **2011**, *17*, 8524-8528.

(26) During the course of the reaction, white precipitate was formed at the beginning of the reaction. After collecting the white precipitate by filtration, the precipitate was assigned to be trichloroacetamide by NMR and mass spectroscopy. The control experiment by adding extra trichloroacetamide (1 equiv.) to the reaction of **2a** with **3a** catalyzed by (*R*)-**1a** resulted in little difference in yield and % ee between the control and the original data. This result suggests that the generated trichloroacetamide does not involve into the catalytic reaction. Therefore involvement of trichloroacetamide in the reaction was not considered in DFT studies.

(27) Frisch, M. J.; *et al. Gaussian 09, Revision C.01*; Gaussian, Inc.: Wallingford, CT, 2010. See SI for the full citation.

(28) For the B97D method, see: Grimme, S. *J. Comput. Chem.* **2006**, *27*, 1787-1799.

(29) For Gaussian basis sets, see: (a) Frisch, M. J.; Pople, J. A.; Binkley, J. S. *J. Chem. Phys.* **1984**, *80*, 3265-3269. (b) Hehre, W. J.; Radom, L.; Schleyer, P. v. R.; Pople, J. A. *Ab initio Molecular Orbital Theory*; John Wiley: New York, USA, 1986, and references cited therein.

(30) (a) Barone, V.; Cossi, M. *J. Phys. Chem. A* **1998**, *102*, 1995-2001. (b) Barone, B.; Cossi, M.; Tomasi, J. *J. Comput. Chem.* **1998**, *19*, 404-417.

(31) The direct displacement of trichloroacetimidate by phosphoric acid catalyst via S_N2 reaction, affording phosphate ester as the reactive intermediate, was also considered as the plausible pathway. However, in general, the S_N2 reaction is significantly influenced by the steric congestion around the reaction site. In fact, substrate **2a** has the sterically hindered tetrasubstituted carbon next to the reaction site. This steric congestion, namely the neopentyl effect on the S_N2 reaction, prevents the proposed S_N2 reaction. Therefore it is considered that the proposed reaction pathway is unfavorable.

(32) Structural optimization of chair-equatorial conformation models was initially conducted using B3LYP/6-31G(d,p), because error occurred when optimization of these equatorial models using the B97D/6-31G(d,p) method. The preliminarily calculations of these equatorial models at the B3LYP/6-31G(d,p) resulted in a conformational change in 1,3-dithiane from the chair forms to the boat-like ones. Further optimization of these boat-axial conformation models was carried out at the B97D/6-31G(d,p) method to afford the corresponding transition states, **TS-1-equatrial-in** and **TS-1-equatrial-out**. Regarding the B3LYP method, see: (a) Becke, A. D. *J. Chem. Phys.* **1993**, *98*, 5648-5652. (b) Lee, C.; Yang, W.; Parr, R. G. *Phys. Rev. B* **1988**, *37*, 785-789.

(33) (a) Desiraju, G. R.; Steiner, T. *The Weak Hydrogen Bond*; Oxford University Press: Oxford, 1999. (b) Castellano, R. K. *Curr. Org. Chem.* **2004**, *8*, 845-865. (c) Knowles, R. R.; Jacobsen, E. N. *Proc. Natl. Acad. Sci. U. S. A.* **2010**, *107*, 20678−20685. (d) Johnston, R. C.; Cheong, P. H.-Y. *Org. Biomol. Chem.* **2013**, *11*, 5057-5064.

(34) For representative and recent examples for C-H···O hydrogen bonds as the key interaction in asymmetric catalysis, see: (a) Corey, E. J.; Rohde, J. J. *Tetrahedron Lett.* **1997**, *38*, 37–40. (b) Grayson. M. N.; Goodman, J. M. *J. Am. Chem. Soc.*, **2013**, *135*, 6142-6148. (c) Maity, P.; Pemberton, R. P.; Tantillo, D. J.; Tambar, U. K. *J. Am. Chem. Soc.* **2013**, *135*, 16380-16383. (d) Wang, H.; Jain, P.; Antilla. J. C.; Houk, K. N. *J. Org. Chem.*, **2013**, *78*, 1208-1215. (e) Ishii, T.; Watanabe, R.; Moriya, T.; Ohmiya, H.; Mori, S.; Sawamura, M. *Chem. Eur. J.* **2013**, *19*, 13547-13553. (f) Grimblat, N.; Sugiura, M.; Pellegrinet, S. C. *J. Org. Chem.* **2014**, *79*, 6754-6758. (g) Xie, Y.; Cheng, G.-J.; Lee, S.; Kaib, P. S. J.; Thiel, W.; List, B. *J. Am. Chem. Soc.* **2016**, *138*, 14538-14541. (h)Lovie-Toon, J. P.; Tram, C. M.; Flynn, B. L.; Krenske, E. H. *ACS Catal.* **2017**, *7*, 3466-3476. (i) Grayson, M. N.; Yang, Z.; Houk, K. N. *J. Am. Chem. Soc.* **2017**, *139*, 7717-7720. (j) Takayama, Y.; Ishii, T.; Ohmiya, H.; Iwai, T.; Schwarzer, M. C.; Mori, S.; Taniguchi, T.; Monde, K.; Sawamura, M. *Chem. Eur. J.* **2017**, *23*, 8400-8404.

(35) *Organic Chemistry of Sulfur*; Oae, S., Eds.; Springer US, 1977.

(36) Seminal works and review about Felkin-Anh model, see: (a) Cherest, M.; Felkin, H.; Prudent, N. *Tetrahedron Lett.* **1968**, *9*, 2199-

2204. (b) Anh, N. T.; Eisenstein, O.; Lefour, J-M.; Dâu, M-E. T. H. *J. Am. Chem. Soc.* **1973**, *95*, 6146-6147. (c) Anh, N. T.; Eisenstein, O. *Tetrahedron Lett.* **1976**, *17*, 155-158. (d) Anh, N. T.; Eisenstein, O. *Nouv. J. Chim.* **1977**, *1*, 61-70. (e) Houk, K. N.; Paddon-Row, M. N.; Rondan, N. G.; Wu, Y.-D.; Brown, F. K.; Spellmeyer, D. C.; Metz, J. T.; Li, Y.; Loncharich, R. J. *Science* **1986**, *231*, 1108-1117. (f) Mengel, A.; Reiser, O. *Chem. Rev*. **1999**, *99*, 1191-1223.

(37) The formation of the present association through the C-H···O hydrogen bonds could be one of the plausible mechanisms of the S_Ni reaction pathway *via* a stepwise process, although covalently bonded phosphate intermediate **INT-3** or **INT-3'** was not detected during the course of the reaction.

(38) We calculated ee value as follows: $\mathrm{ee} = \frac{\exp\left(\frac{\Delta\Delta G^{TS}}{RT}\right)-1}{\exp\left(\frac{\Delta\Delta G^{TS}}{RT}\right)+1}$.

where $\Delta\Delta G^{TS}$ is the energy gap between major and minor transition states, R is gas constant, and T is absolute temperature. The 2.6 kcal/mol energy gap at -40 ºC corresponds to 99% ee. However, the experimental result using **2k** is 96% ee.

(39) For C-H···π interaction, see: (a) Krenske, E. H.; Houk, K. N. *Acc. Chem. Res.* **2013**, *46*, 979-989. (b) Neel, A. J.; Hilton, M. J.; Sigman, M. S.; Toste, F. D. *Nature* **2017**, *543*, 637-646.

(40) For representative and recent examples for C-H···π as the key interaction in asymmetric catalysis, see: (a) Yamakawa, M.; Yamada, I.; Noyori, R. *Angew. Chem. Int. Ed.* **2001**, *40*, 2818–2821. (b) Dang, Y.; Qu, S.; Wang, Z.-X.; Wang, X. *J. Am. Chem. Soc*. **2014**, *136*, 986-998. (c) Jindal, G.; Sunoj, R. B. *Angew. Chem., Int. Ed*. **2014**, *53*, 4432-4436. (d) Meng, S. S.; Liang, Y.; Cao, K. S.; Zou, L.; Lin, X. B.; Yang, H.; Houk, K. N.; Zheng, W. H. *J. Am. Chem. Soc*. **2014**, *136*, 12249-12252. (e) Bhaskararao, B.; Sunoj, R. B. *J. Am. Chem. Soc*. **2015**, *137*, 15712-15722. (f) Changotra, A.; Sunoj, R. B. *Org. Lett*. **2016**, *18*, 3730-3733. (g) Doney, A. C.; Rooks, B. J.; Lu, T. X.; Wheeler, S. E. *ACS Catal*. **2016**, *6*, 7948-7955. (h) Pareek, M.; Sunoj, R. B. *ACS Catal*. **2016**, *6*, 3118-3126. (i) Korenaga, T.; Sasaki, R.; Takemoto, T.; Yasuda, T.; Watanabe, M. *Adv. Synth. Catal*. **2018**, *360*, 322-333.

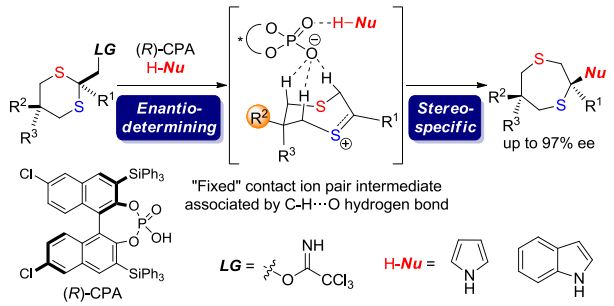
LG
(R)-CPA
H-Nu
Enantio-determining
Stereo-specific
Nu
up to 97% ee
"Fixed" contact ion pair intermediate
associated by C-H···O hydrogen bond
(R)-CPA
LG =
H-Nu =